Influence of Polyelectrolyte Multilayer Coatings on Förster Resonance Energy Transfer between 6-Carboxyfluorescein and Rhodamine B-Labeled Particles in Aqueous Solution

Frank Caruso,* Edwin Donath, and Helmuth Möhwald

Max-Planck-Institute of Colloids and Interfaces, Rudower Chaussee 5, D-12489 Berlin, Germany

Received: November 13, 1997; In Final Form: January 22, 1998

The Förster resonance energy transfer (FRET) between 6-carboxyfluorescein (6-CF) (donor) and rhodamine B-labeled melamine formaldehyde (RhB-MF) particles (acceptor) in aqueous solution was exploited to investigate the layer properties of polyelectrolyte (PE) multilayers preadsorbed on the particle surface. The formation of poly(styrenesulfonate) (PSS) and poly(allylamine hydrochloride) (PAH) multilayers on the RhB-MF particles was confirmed by electrophoretic mobility measurements. The FRET process was found to proceed via adsorption of 6-CF onto the RhB-MF particles and was thus dependent on the degree of surface coverage of the PE on the surface. The PE surface coverage could be altered by depositing the layers with or without added electrolyte. The extent of FRET was also influenced by the number of PE layers (and hence layer thickness) surrounding the RhB-MF particles. Increasing the number of PE layers resulted in less energy transfer, reflecting less accessible sites on the RhB-MF particles for 6-CF adsorption. The PE layers were found to be permeable to 6-CF, with no diffusion effects evident on the time scale of the steady-state fluorescence measurements. Further, 6-CF was found to interact with PAH when the outer PE layer on the particles was PAH. This interaction presents a novel way of detecting amino sites of PAH not interacting with PSS in the PE multilayer films.

Introduction

The layer-by-layer (LBL) self-assembly technique has attracted much attention recently because of its simplicity, versatility, and effectiveness in preparing ultrathin polyelectrolyte multilayer films on solid surfaces.[1−14] The LBL method, which involves the sequential adsorption of oppositely charged polymeric molecules from dilute solution, is particularly useful in that it allows the structure, composition, and thickness of the film to be controlled. In addition, highly ordered and uniform multilayer assemblies on solid substrates are formed. Although the LBL technique was originally introduced for the formation of PE multilayers, it has recently been extended to the self-assembly of other charged species, alternating with a polyion, to fabricate multilayer films. Charged species ranging from biomolecules, such as proteins[15−19] and nucleic acids,[20−23] to low molecular weight dye molecules,[25−29] and to various inorganic particles[30−39] have been included in PE films. These films have promising technological applications in the areas of sensors, microelectronics, catalysis, and nonlinear optics.

The vast majority of studies on the fabrication of supramolecular assemblies using the LBL technique have employed macroscopic flat (charged) substrates as the initial surface for the layer buildup. Recently, however, the technique has been applied to form PE multilayers on micron-sized charged polystyrene latex particles.[40] It was demonstrated that PE multilayer-coated particles with controlled thickness, composition, and charge can be produced.[40] Analogous to the exploitation of PE multilayers on macroscopic flat substrate surfaces, it should also be possible to incorporate functional charged species within polyion layers formed on colloidal particles. This is of particular interest in the biomedical field where, in diagnostic tests, latex particles are widely used as solid supports for the immobilization of various biomolecules (antibodies, enzymes, DNA).[41−44] In addition, such PE multilayer-coated particles are envisaged to have potential as microcarriers or microreactors. An understanding of the layer properties of PE multilayer films is important if the layer-by-layer assembly method is to be optimized for the preparation of functional films where, for example, certain biochemical species need to permeate into the film to interact with specific species immobilized within the layers.[19,23]

The present study investigates the layer properties of PE multilayers coated on micron-sized particles (Figure 1) via the extent of Förster resonance energy transfer (FRET) between the donor, 6-carboxyfluorescein (6-CF), and acceptor, rhodamine B-labeled melamine formaldehyde (RhB-MF) particles, in aqueous solution. The layer-by-layer assembly of PSS and PAH was followed by electrophoresis measurements. The effects of PE layer number and surface coverage on the degree of FRET, as well as the permeability of the PE layers to 6-CF, have been examined. It is also shown that when the outer layer of the PE film is PAH, the charged amino groups of PAH not utilized in the layer buildup with PSS and that are accessible interact with 6-CF.

Experimental Section

Materials. Anionic poly(sodium 4-styrenesulfonate) (PSS), M_r 70 000, and cationic poly(allylamine hydrochloride) (PAH), M_r 8000−11 000, were obtained from Aldrich. Before use, PSS was dialyzed against Milli-Q water (MW cutoff 14 000) and lyophilized. 6-Carboxyfluorescein was obtained from Sigma and used as supplied. Positively charged homogeneously doped

* To whom correspondence should be addressed: Fax +49 30 6392 3102; E-mail caruso@mpikg.fta-berlin.de.

S1089-5647(98)00198-9 CCC: $15.00
Published on Web 02/24/1998

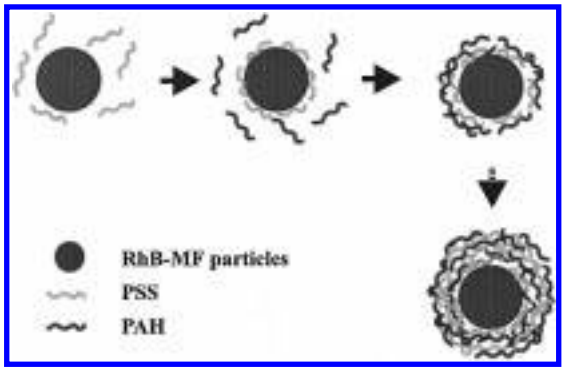

Figure 1. Schematic of the assembly of polyelectrolytes onto positively charged RhB-MF particles. The polyelectrolyte multilayer film is formed by the alternate adsorption of oppositely charged polyelectrolytes. The first adsorption step is that of PSS, followed by PAH. After each adsorption step the polyelectrolyte is removed by repeated centrifugation/washing cycles. By repeating this procedure, the desired number of polyelectrolyte layers can be deposited.

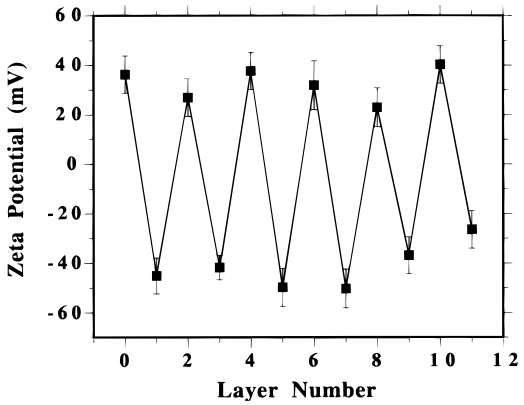

Figure 2. ζ-potential as a function of PE layer number for PSS/PAH-coated positively charged RhB-MF particles. The odd layer numbers correspond to PSS deposition and the even layer numbers to PAH deposition.

RhB-MF particles of diameter 3.35 μm were purchased from Microparticles, GmbH. Sodium chloride (AR grade) was purchased from Merck and used as received. The water used in all experiments was prepared in a three-stage Millipore Milli-Q Plus 185 purification system and had a resistivity higher than 18.2 MΩ cm.

Polyelectrolyte Multilayer Film Formation on RhB-MF Particles. A 0.4 mL aliquot of an aqueous 1 mg mL^{-1} PSS solution containing 0.5 M NaCl was added to 0.1 mL of the positively charged RhB-MF particles (3.5 wt %) in a 2 mL Eppendorf tube. The RhB-MF particles were allowed to interact with the PE solution for 20 min with occasional stirring of the dispersion. The dispersion was then centrifuged at 2000 rpm for 5 min, the supernatant was removed, 1.5 mL of water was added, and the particles were redispersed by gentle shaking. The centrifugation/wash/redispersion cycle was repeated a further three times. The supernatant was then removed, and 0.4 mL of an aqueous 1 mg mL^{-1} PAH solution containing 0.5 M NaCl was added to the PSS-coated RhB-MF particles. The adsorption time allowed was again 20 min. The same procedure, as described above, was followed for deposition of this PAH layer and for additional PE layers. The PE concentrations used for the multilayer assembly were larger than those required for adsorption saturation of the surfaces. Polyelectrolyte adsorption times of 20 min were sufficient for adsorption saturation, as evidenced by the ζ-potential values; longer adsorption times had no effect on the ζ-potential values.

Electrophoretic Mobility (EM) Measurements. Electrophoretic mobilities of the RhB-MF particles were measured using a Malvern Zetasizer 4. The mobility u was converted into a ζ-potential using the Smoluchowski relation ($\zeta = u\eta/\epsilon$, where η and ϵ are the viscosity and permittivity of the solution, respectively). All ζ-potential measurements were performed in pure water.

Steady-State Fluorescence Measurements. Fluorescence measurements were carried out using a Spex Fluorolog 1680 spectrometer. The excitation wavelength ($\lambda_{ex} = 450$ nm) was chosen to excite the donor (6-CF) and to minimize absorption by the acceptor (RhB-MF particles). The emission spectra were recorded in the range 480−700 nm. Both excitation and emission bandwidths were set at 1.0 nm.

Since the preparation of PE multilayer coated RhB-MF particles involved a number of centrifugation/redispersion cycles, some of the particles were inevitably lost in the process. Thus, the concentration of the RhB-MF particles in each sample was adjusted until an arbitrarily chosen fluorescence intensity value at 595 nm was attained (corresponding to ca. 0.2 wt % of particles). (Although it is difficult to measure absolute intensities from colloidal dispersions, it was found that the above method consistently yielded similar FRET curves, indicating a negligible variation in the total number of particles.) Typically, ca. 10−20 μL of the particles was pipetted into approximately 2 mL of water in a fluorimeter cell and the dispersion agitated for 0.5 min. The fluorescence spectrum of the RhB-MF sample was then recorded. Aliquots of 6-CF were subsequently added, the dispersion was gently stirred, and the fluorescence spectrum was recorded. This procedure was repeated for different concentrations of 6-CF. FRET from the 6-CF to RhB-MF particles was evidenced by an increase in the fluorescence intensity at 595 nm. These experiments were repeated using RhB-MF particles coated with different numbers of PE layers.

6-CF Adsorption onto RhB-MF Particles. The number of RhB-MF particles in 20 mL of water was adjusted to give an arbitrarily chosen value (equivalent to that of the other samples used in the FRET experiments) for the fluorescence of RhB-MF at 595 nm. Aliquots of 6-CF were subsequently added to the RhB-MF particle sample and also to a blank (20 mL of water). Adsorption was allowed to proceed for 10 min. (FRET experiments show this time is sufficient for equilibrium adsorption of 6-CF onto the RhB-MF particles.) A 1 mL aliquot of the sample was then removed, placed in an Eppendorf tube, and centrifuged at 5500 rpm for 5 min. Following this, 0.5 mL of the supernatant was removed and added to a cuvette cell containing 1 mL of phosphate buffer (pH 7, Riedel-de Haën) and 0.5 mL of water. (The phosphate buffer was used to avoid any pH effects on the 6-CF fluorescence intensity.) Similarly, 0.5 mL of the blank solution was removed and added to a cuvette containing 1 mL of phosphate buffer and 0.5 mL of water. The fluorescence spectra of the blank and sample were taken. The amount of 6-CF adsorbed onto the RhB-MF particles was determined from the difference in the fluorescence between the blank and sample at 515 nm. The amount of 6-CF adsorbed was then plotted as a function of the equilibrium 6-CF concentration in solution.

Results and Discussion

Figure 2 shows the ζ-potential values as a function of PE layer number for RhB-MF particles coated with PSS/PAH multilayers. The positive ζ-potential of the uncoated RhB-MF particles (ca. +35 mV) is consistent with a positively charged particle surface. The presence of PSS, which is anionic,

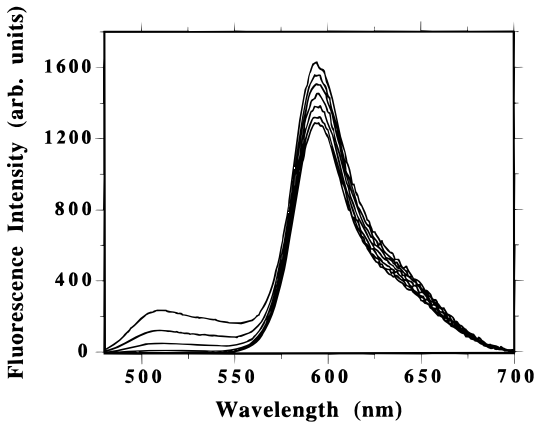

Figure 3. Fluorescence spectra of uncoated RhB-MF particles in the presence of different 6-CF concentrations. Spectra (from bottom to top): 0, 50, 100, 196, 338, 520, and 740 nM 6-CF. Excitation wavelength = 450 nm.

causes a reversal in ζ-potential to ca. −45 mV. Subsequent deposition of PAH onto the PSS-coated RhB-MF particles once again reverses the ζ-potential, the value being ca. +25 mV. The deposition of additional (up to 11) layers yields alternating ζ-potentials. Since the conformation of the PE on the surface may alter the magnitude of the ζ-potential, no quantitative conclusions are drawn from the ζ-potential data. The observed alternating ζ-potential with layer number, however, qualitatively demonstrates that regular stepwise PSS/PAH multilayer growth occurs on the RhB-MF particles. It has recently been demonstrated that the formation of PAH/PSS multilayers on negatively charged polystyrene latex particles also results in alternating ζ-potential values with increasing layer number.[40] In that work, an increase in thickness of the multilayer film with each PE layer deposited was also reported.[40] It is not possible to determine the PE layer thicknesses on the RhB-MF particles using the technique of single particle light scattering (SPLS)[40] because of complicated scattering functions due to the large size of the particles. SPLS measurements, however, reveal that no significant aggregation of the PE-coated RhB-MF particles occurs.

Fluorescence experiments were first performed using uncoated RhB-MF particles and 6-CF to investigate the FRET process. Figure 3 shows the fluorescence spectra of uncoated RhB-MF particles (λ_{ex} = 450 nm) in the absence of the donor 6-CF (bottom spectrum) and in the presence of different amounts of 6-CF. At the excitation wavelength of 450 nm, the absorbance of 6-CF is at a maximum, whereas that of RhB-MF is low (λ_{max} = 590 nm). The fluorescence spectrum of the uncoated RhB-MF particles in the absence of 6-CF exhibits a fluorescence maximum at 595 nm. The addition of 6-CF to the RhB-MF sample produces an increase in acceptor fluorescence intensity at 595 nm, as well as a broad emission band centered around 515 nm, corresponding to 6-CF in solution. The spectra in Figure 3 clearly illustrate that, at low (<200 nM) 6-CF concentrations, where emission from 6-CF in solution is small, there is a noticeable increase in the acceptor fluorescence at 595 nm. This observation is consistent with FRET; the donor fluorescence is quenched by transferring energy to the acceptor.

The effect of 6-CF in solution to the FRET process is negligible. The number of 6-CF molecules contributing to FRET by pure diffusion into the Förster distance (5.1 nm[45]) is approximately 6 orders of magnitude less than that in bulk solution and thus cannot be detected against the background of the bulk 6-CF fluorescence. Further, at the 6-CF concentrations used (less than 1 μM), fluorescence self-quenching of 6-CF in solution can be ruled out.[46] These observations suggest that 6-CF adsorbs onto the surface of the RhB-MF particles and/or that there is an enrichment of 6-CF near the surface of the particles, allowing FRET to occur. To investigate this, we studied the adsorption of 6-CF onto the positively charged RhB-MF particles.

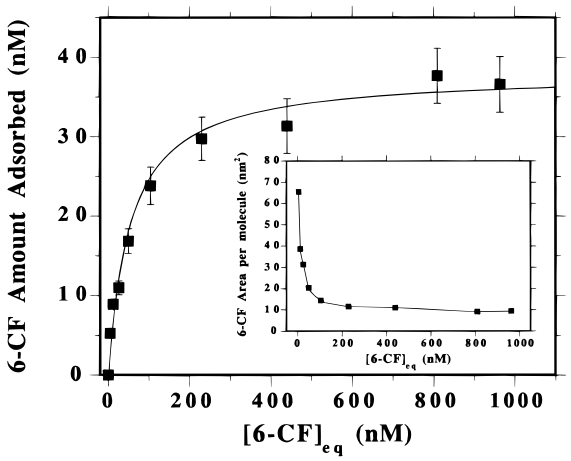

Figure 4. Adsorption isotherm of 6-CF from water onto the RhB-MF particles. The curve represents a Langmuir fit to the experimental data. The inset shows the area per molecule for 6-CF on the RhB-MF particles as a function of 6-CF equilibrium concentration.

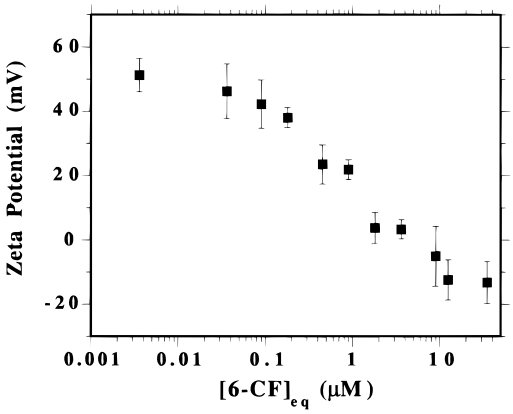

Figure 5. ζ-potential of RhB-MF particles exposed to 6-CF as a function of 6-CF equilibrium concentration.

The adsorption isotherm of 6-CF from water onto the RhB-MF particles is shown in Figure 4. The curve is a theoretical Langmuir fit to the experimental data. The maximum amount of 6-CF adsorbed onto the RhB-MF particles obtained from the Langmuir fit is 38 ± 5 nM, representing saturation coverage of the surface. The adsorption constant is calculated to be (1.7 ± 0.2) × 10^7 M^{-1}. The inset in Figure 4 shows the corresponding area per molecule values for 6-CF on the RhB-MF particles plotted as a function of the 6-CF equilibrium concentration. At saturation coverage the minimum area per molecule occupied by each 6-CF molecule is 10 nm^2. In arriving at this value, we have assumed that the surface of the RhB-MF particles is smooth. Since the RhB-MF particles are composed of polymeric material, their surface area is expected to be larger (due to surface roughness) than that calculated for a perfectly smooth particle. Thus, the value of 10 nm^2 represents a lower limit. The minimum mean free distance between 6-CF molecules is calculated as 3 nm.

To further examine the adsorption of 6-CF onto the RhB-MF particle surface, electrophoretic mobility (EM) measurements were performed. Figure 5 shows the ζ-potential values for RhB-MF particles exposed to 6-CF as a function of the 6-CF

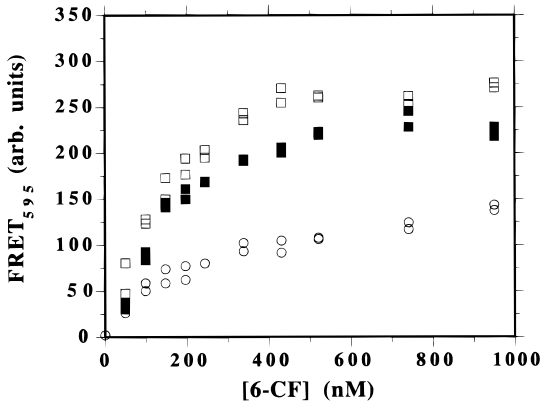

Figure 6. FRET at 595 nm for RhB-MF particles as a function of 6-CF concentration: filled squares, uncoated RhB-MF particles; open squares, PSS-coated RhB-MF particles, PSS layer deposited from 0.5 M NaCl solution; circles, PSS-coated RhB-MF particles, PSS layer deposited from an aqueous solution containing no added electrolyte. Data for two separate experiments are shown for each system. See text for details concerning calculation of the degree of FRET.

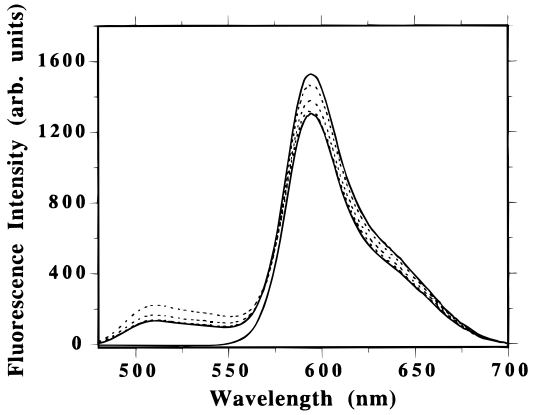

Figure 7. Effect of PSS on the fluorescence spectrum of uncoated RhB-MF particles previously exposed to a 390 nM 6-CF solution. Lower spectrum: uncoated RhB-MF particles. Top spectrum (at 595 nm): 6-CF coated RhB-MF particles. Dashed spectra (from top to bottom at 595 nm): 6-CF coated RhB-MF particles exposed to PSS concentrations of 2.0×10^{-5}, 6.4×10^{-4}, and 7.7×10^{-2} mg mL^{-1}, respectively.

equilibrium concentration. (In the EM experiments the number of RhB-MF particles used was 1000 times smaller than the number used in the adsorption isotherm experiments. The amount of 6-CF adsorbed is therefore negligible, and the total 6-CF concentration is assumed equal to the free 6-CF concentration.) Figure 5 shows that there is a decrease in ζ-potential in the 6-CF concentration range $0-1$ μM, reflecting adsorption of 6-CF onto the particle surface. This is in agreement with the adsorption isotherm data presented in Figure 4. The further change of ζ-potential beyond the concentration range of 1 μM may occur as a result of ionic strength changes with each 6-CF addition. It should also be noted that electrophoretic mobility values are mostly influenced by the outer charges of the particles, and adsorption of 6-CF into deeper regions of the particles (i.e., in pores) would contribute less to the ζ-potential values. Hence, although the data in Figure 5 qualitatively indicate that 6-CF adsorption onto the particles occurs, the ζ-potential values may not *accurately* reflect the charge density present on the particles as a result of 6-CF adsorption.

Having established that 6-CF adsorbs onto the surface of the RhB-MF particles, resulting in FRET, the effect of PE layers on the FRET transfer process was then studied. In the first instance the influence of one PSS layer deposited onto the positively charged RhB-MF particles from solutions with or without added electrolyte was investigated. Figure 6 shows the fluorescence intensity due to FRET at 595 nm ($FRET_{595}$) as a function of the 6-CF concentration for uncoated RhB-MF particles (data from Figure 3), and for RhB-MF particles coated with one PSS layer, deposited from either a 0.5 M NaCl solution or an aqueous solution containing no added electrolyte. Fluorescence from 6-CF in solution contributes to that of the RhB-MF particles (particularly at higher 6-CF concentrations). The extent of $FRET_{595}$ was therefore calculated from the difference in the fluorescence intensities of the RhB-MF particles in the presence and absence of 6-CF at 595 nm, allowing for the contribution to the fluorescence intensity at 595 nm from 6-CF in solution. (For 6-CF in solution the fluorescence intensity at 595 nm is ca. 40% of that at 515 nm.)

From Figure 6 it can be seen that the FRET values are reproducible; data for two separate experiments are shown for each system. The degree of FRET for the uncoated particles is seen to increase most rapidly at low 6-CF concentrations and plateaus after 6-CF concentrations of approximately 500 nM. Similar shape curves are obtained for the particles coated with one PSS layer. The FRET plateau value of ca. 500 nM is close to the saturation concentration found in the 6-CF adsorption isotherm (Figure 4). This is consistent with 6-CF adsorption onto the RhB-MF particles being responsible for FRET. The rate of increase of FRET with concentration (Figure 6) is slightly smaller than the rate of increase of the 6-CF adsorbed amount with concentration shown in Figure 4. This could be due to the presence of 6-CF self-quenching in the FRET experiments.

The extent of FRET for the RhB-MF particles coated with PSS from solutions containing 0.5 M NaCl is marginally higher than that of the uncoated RhB-MF particles. This may indicate that the mean distance of 6-CF is increased due to the presence of PSS on the surface, resulting in less 6-CF self-quenching. It may also be possible that the nature of the surface, due to PSS being present, has an influence on the FRET process. A more noticeable difference is seen for the FRET data for particles with PSS deposited from solutions containing no added electrolyte. Here, the extent of FRET is significantly reduced. This is attributed to PSS adopting a flat conformation in the absence of electrolyte (since the electrolyte screens the electrostatic repulsion between the ionic groups on the chains of PSS[4,47]), thereby reducing the area available for 6-CF adsorption and hence the degree of FRET. In addition, in the absence of electrolyte there is reduced shielding of charges in PSS. This may result in a stronger attraction of PSS for the positively charged RhB-MF particles, which may in turn indicate that the *charged* sites on the particles are important for the adsorption of 6-CF. Further evidence that the number of sites available for 6-CF adsorption affects FRET comes from the observation that all three curves in Figure 6 can be scaled to fit a single curve. This suggests that the mechanism of 6-CF adsorption is the same and that only the number of sites available for adsorption is different.

The effect of PSS (containing no added electrolyte) on the fluorescence spectrum (and FRET) of RhB-MF particles previously exposed to a solution of 390 nM 6-CF is demonstrated in Figure 7. The concentrations of PSS corresponding to the three dashed spectra, from top to bottom at 595 nm, are 2.0×10^{-5}, 6.4×10^{-4}, and 7.7×10^{-2} mg mL^{-1}, respectively. The fluorescence spectrum for the uncoated RhB-MF particles (lower spectrum) is also shown for comparison. As in Figure 3, the fluorescence intensity at 595 nm is enhanced by FRET when 6-CF is adsorbed onto the particles, and a broad peak due to

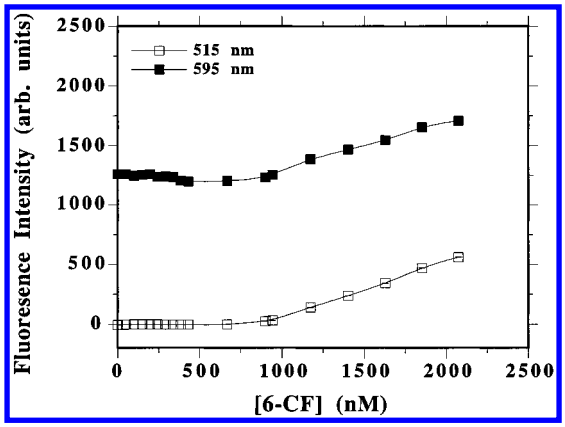

Figure 8. Fluorescence intensity at 595 nm (corresponding to FRET) and at 515 nm (corresponding to 6-CF in bulk solution) as a function of added 6-CF concentration for (PSS/PAH)-coated RhB-MF particles. PE layers were deposited from solutions containing 0.5 M NaCl.

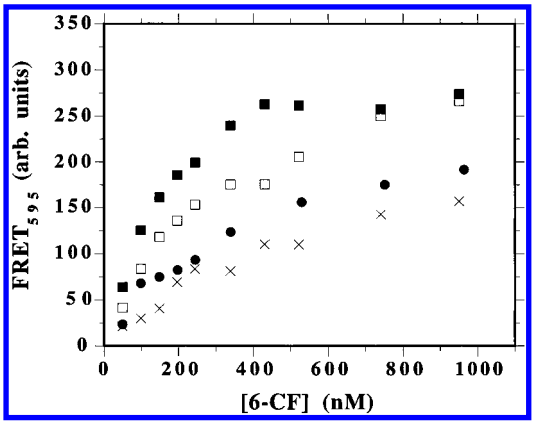

Figure 9. FRET at 595 nm for alternating PSS/PAH multilayer-coated RhB-MF particles as a function of 6-CF concentration: filled squares, 1 layer PSS; open squares, 5 layers; circles, 9 layers; crosses, 11 layers. PE layers were deposited from solutions containing 0.5 M NaCl. Each data point represents the average of two repeat experiments. See text for details concerning calculation of the degree of FRET.

6-CF in solution centered around 515 nm is seen. Upon adding PSS, the fluorescence intensity at 595 nm decreases while the broad peak around 515 nm increases. This is clear evidence that PSS replaces 6-CF adsorbed on the RhB-MF particles, liberating 6-CF into solution and reducing the degree of FRET.

RhB-MF particles coated with two PE layers, first PSS and second PAH, were prepared. Figure 8 shows the fluorescence intensity values at the maximum wavelength where FRET occurs (595 nm), and at the maximum of 6-CF fluorescence (515 nm), as a function of 6-CF concentration for (PSS/PAH)-coated RhB-MF particles. Figure 8 reveals that at low 6-CF concentrations there is no increase in fluorescence intensity at 595 nm, nor is there an increase at 515 nm. At 6-CF concentrations above about 550 nM there is an increase in fluorescence intensity for both wavelengths. Beyond this concentration FRET occurs—similar FRET data (within experimental error) to that observed for PSS-coated RhB-MF particles (Figure 6) are obtained. The above data suggest that at low concentrations 6-CF is not adsorbed directly on the RhB-MF particle surface, which would result in FRET, nor is it in bulk solution. Rather, the data indicate that there is strong interaction between 6-CF and PAH, when PAH forms the outer layer. In this situation, the cationic PAH effectively provides a positively charged surface (replacing that of the RhB-MF particles) for adsorption of the anionic 6-CF. (The interaction between 6-CF and PAH most probably proceeds as a result of electrostatic attraction.) This allows "titration" of the free charged (amino) sites of PAH which do not interact with the underneath PSS layer and which are accessible to 6-CF. (The interaction between PSS and PAH is stronger than the probe−polyelectrolyte interaction.) Using the 6-CF concentration that represents "maximum titration" of the PAH layer (550 ± 50 nM), the number of titrated sites per nm^2 is estimated as 1.60 ± 0.15. The area per monomer in PAH obtained from theoretical calculations is 0.27 nm^2,[48] corresponding to 3.6 PAH monomers per nm^2 if monolayer coverage is assumed. Accurate evaluation of the number of 6-CF molecules per PAH monomer is, however, not possible since the layer thickness and hence the amount of polyelectrolyte on the RhB-MF colloids could not be determined (see earlier). Although it has been reported that a 1:1 stoichiometry may exist between oppositely charged PEs in multilayer assemblies (i.e., every charge on a polycation is compensated by a charge on a polyanion), no information on the number of charged sites in a given PE compensated by each surrounding layer is given.[12] The above 6-CF/PAH interaction presents a new way of examining the electrostatic interactions in multilayer films via the number of groups participating in the layer-by-layer assembly. Detailed evaluation of this interaction and that of other probe molecules with various PEs (including PAH) in PE multilayers, as studied by fluorescence spectroscopy, will appear in a subsequent paper.[49]

The addition of PSS (2.4×10^{-2} mg mL^{-1}, no added electrolyte) to a sample of (PSS/PAH)-coated RhB-MF particles that were previously exposed to 6-CF (at a concentration of 500 nM) results in PSS adsorbing onto the PAH, releasing 6-CF into solution (data not shown). The 6-CF released into solution then adsorbs onto the surface of the particles causing FRET to occur. The above situation is similar to the process observed in Figure 7 where PSS displaces 6-CF from the RhB-MF particle surface.

Due to the interaction observed for 6-CF with PAH, the FRET process was investigated for RhB-MF particles coated with varying odd numbers of PE multilayers, that is, with PSS forming the outer layer. The FRET data as a function of 6-CF concentration for RhB-MF particles coated with 1, 5, 9, or 11 alternating PSS/PAH multilayers are shown in Figure 9. The data in Figure 9 clearly reveal that there is a decrease in the extent of FRET with an increase in the number of PE layers on the RhB-MF particles. The possibility that there are PAH sites in the multilayer films that influence the FRET data can be ruled out because experiments involving PE layers formed on particles that do not adsorb 6-CF (negatively charged polystyrene latex particles) reveal that no probe adsorption occurs onto the layers provided the outer layer is PSS. This suggests that there are no PAH sites interacting with 6-CF in the multilayer films when PSS forms the outermost layer.

It was earlier established that the degree of FRET is dependent on the RhB-MF particles surface area available for 6-CF adsorption (see Figure 6). Equilibrium conditions were approached within the time frame of the experiments (ca. 2 min), indicating that diffusion is not the limiting step. The results can therefore be interpreted in terms of the number of accessible 6-CF binding sites. The decrease in the FRET plateau value with increasing layer number on the RhB-MF particles suggests that the number of accessible binding sites for 6-CF decreases. The decrease in the FRET efficiency with increasing PE layer number may be explained by the additional layers altering the surface conformation, and hence the area occupied, of the layers beneath them. Incoming PSS may also penetrate preadsorbed layers and occupy area on the particles. The FRET data also

show the general trend that the 6-CF concentration required to attain the FRET plateau value increases with increasing layer number on the particles. This could be explained by an overall decreased binding constant for 6-CF; some binding sites in the vicinity of adsorbed polyelectrolyte may have a decreased binding affinity.

The PE layers studied are readily permeated by small molecules such as 6-CF. The ability of 6-CF to permeate the PE layers was not influenced by the PE layer number (between 1 and 11 layers) when PSS formed the outer layer. This was examined by following the FRET process with time. Recent atomic force microscopic measurements confirm that PE PAH/PSS multilayer films formed on solid substrates contain regions large enough for small molecules such as 6-CF to permeate the layers.[50]

Conclusions

We have shown that the layer-by-layer assembly technique can be used to successfully form PE multilayers on micron-sized RhB-MF particles. It has also been established that Förster resonance energy transfer can be used to study various properties of PE multilayers coated on RhB-MF particles: (i) the accessibility of 6-CF to surface sites within the PEs and on the particle surface and (ii) the permeability of 6-CF through PE multilayers. The number of sites available for 6-CF binding on the particles is influenced by the PE conformation on the surface and the number of PE layers on the particles. Permeation of the layers by 6-CF was found to be unaffected by the PE layer number within the time scale of the experiments. Further, the amino groups in PAH assembled in the multilayer films were identified as binding sites for 6-CF, with FRET occurring only after saturation of these sites. This study has provided information on the properties of PE multilayers and may aid in optimizing the design of functional supramolecular assemblies constructed using the layer-by-layer assembly technique.

Acknowledgment. Frank Caruso acknowledges the Alexander von Humboldt Foundation for a Research Fellowship.

References and Notes

(1) Decher, G.; Hong, J. D. *Makromol. Chem., Macromol. Symp.* **1991,** *46,* 321.
(2) Decher, G.; Hong, J. D. *Ber. Bunsen-Ges. Phys. Chem.* **1991,** *95,* 1430.
(3) Decher, G.; Hong, J. D.; Schmitt, J. *Thin Solid Films* **1992,** *210/211,* 831.
(4) Decher, G.; Schmitt, J. *Prog. Colloid Polym. Sci.* **1992,** *89,* 160.
(5) Lvov, Y.; Decher, G.; Möhwald, H. *Langmuir* **1993,** *9,* 481.
(6) Decher, G.; Lvov, Y.; Schmitt, J. *Thin Solid Films* **1994,** *244,* 772.
(7) Ramsden, J. J.; Lvov, Y. M.; Decher, G. *Thin Solid Films* **1995,** *254,* 246.
(8) Ferreira, M.; Rubner, M. F. *Macromolecules* **1995,** *28,* 7107.
(9) Fou, A. C.; Rubner, M. F. *Macromolecules* **1995,** *28,* 7115.
(10) Kellogg, G. J.; Mayes, A. M.; Stockton, W. B.; Ferreira, M.; Rubner, M. F.; Satija, S. K. *Langmuir* **1996,** *12,* 5109.
(11) Fou, A. C.; Onitsuka, O.; Ferreira, M.; Rubner, M. F.; Hsieh, B. R. *J. Appl. Phys.* **1996,** *79,* 7501.
(12) Sukhorukov, G. B.; Schmitt, J.; Decher, G. *Ber. Bunsen-Ges. Phys. Chem.* **1996,** *100,* 948.
(13) Cheung, J. H.; Stockton, W. B.; Rubner, M. F. *Macromolecules* **1997,** *30,* 2712.
(14) Caruso, F.; Niikura, K.; Furlong, D. N.; Okahata, Y. *Langmuir* **1997,** *13,* 3422.
(15) Lvov, Y.; Ariga, K.; Kunitake, T. *Chem. Lett.* **1994,** 2323.
(16) Kong, W.; Zhang, X.; Gao, M.; Zhou, H.; Li, W.; Shen, J. *Macromol. Rapid Commun.* **1994,** *15,* 405.
(17) Lvov, Y.; Ariga, K.; Ichinose, I.; Kunitake, T. *J. Am. Chem. Soc.* **1995,** *117,* 6117.
(18) Onda, M.; Lvov, Y.; Ariga, K.; Kunitake, T. *Biotechnol. Bioeng.* **1996,** *51,* 163.
(19) Caruso, F.; Niikura, K.; Furlong, D. N.; Okahata, Y. *Langmuir* **1997**, *13,* 3427.
(20) Decher, G.; Lehr, B.; Lowack, K.; Lvov, Y.; Schmitt, J. *Biosens. Bioelectron.* **1994,** *9,* 677.
(21) Sukhorukov, G. B.; Möhwald, H.; Decher, G.; Lvov, Y. M. *Thin Solid Films* **1996,** *284/285,* 220.
(22) Sukhorukov, G. B.; Montrel, M. M.; Petrov, A. I.; Shabarchina, L. I.; Sukhorukov, B. I. *Biosens. Bioelectron.* **1996,** *11,* 913.
(23) Caruso, F.; Rodda, E.; Furlong, D. N.; Niikura, K.; Okahata, Y. *Anal. Chem.* **1997,** *69,* 2043.
(24) Ichinose, I.; Fujiyoshi, K.; Mizuki, S.; Lvov, Y.; Kunitake, T. *Chem. Lett.* **1996,** 257.
(25) Cooper, T. M.; Campbell, A. L.; Crane, R. L. *Langmuir* **1995,** *11,* 2713.
(26) Yoo, D.; Wu, A. P.; Lee, J.; Rubner, M. F. *Synth. Met.* **1997,** *85,* 1425.
(27) Araki, K.; Wagner, M. J.; Wrighton, M. S. *Langmuir* **1996,** *12,* 5393.
(28) Ariga, K.; Lvov, Y.; Kunitake, T. *J. Am. Chem. Soc.* **1997,** *119,* 2224.
(29) Ariga, K.; Onda, M.; Lvov, Y.; Kunitake, T. *Chem. Lett.* **1997,** 25.
(30) Kleinfeld, E. R.; Ferguson, G. S. *Science* **1994,** *265,* 370.
(31) Keller, S. W.; Kim, H.-N.; Mallouk, T. E. *J. Am. Chem. Soc.* **1994**, *116,* 8817.
(32) Kotov, N. A.; Dekany, I.; Fendler, J. H. *Adv. Mater.* **1996,** *8,* 637.
(33) Kleinfeld, E. R.; Ferguson, G. S. *Chem. Mater.* **1996,** *8,* 1575.
(34) Ariga, K.; Lvov, Y.; Onda, M.; Ichinose, I.; Kunitake, T. *Chem. Lett.* **1997,** 125.
(35) Kotov, N. A.; Haraszti, T.; Turi, L.; Zavala, G.; Geer, R. E.; Dekany, I.; Fendler, J. H. *J. Am. Chem. Soc.* **1997,** *119,* 6821.
(36) Ichinose, I.; Senzu, H.; Kunitake, T. *Chem. Lett.* **1996,** 831.
(37) Kotov, N. A.; Dekany, I.; Fendler, J. H. *J. Phys. Chem.* **1995,** *99,* 13065.
(38) Feldheim, D. L.; Grabar, K. C.; Natan, M. J.; Mallouk, T. E. *J. Am. Chem. Soc.* **1996,** *118,* 7640.
(39) Schmitt, J.; Decher, G.; Dressick, W. J.; Brandow, S. L.; Geer, R. E.; Shashidhar, R.; Calvert, J. M. *Adv. Mater.* **1997,** *9,* 61.
(40) Sukhorukov, G. B.; Donath, E.; Lichtenfeld, H.; Knippel, E.; Knippel, M.; Möhwald, H. *Colloids Surf., A,* in press.
(41) Arshady, R. *Biomaterials* **1993,** *14,* 5.
(42) Slomkowski, S.; Kowalczyk, D.; Trznadel, M. *Trends Polym. Sci.* **1995,** *3,* 297.
(43) Wolf, S. F.; Haines, L.; Fisch, J.; Kremsky, J. N.; Dougherty, J. P.; Jacobs, K. *Nucleic Acids Res.* **1987,** *15,* 2911.
(44) Charreyre, M.-T.; Tcherkasskaya, O.; Winnik, M. A.; Hiver, A.; Delair, T.; Cros, P.; Pichot, C.; Mandrand, B. *Langmuir* **1997,** *13,* 3103.
(45) Chen, R.; Knutson, J. *Anal. Biochem.* **1988,** *172,* 61.
(46) The fluorescence intensity of 6-CF solutions was found to be linear with 6-CF concentration in the range 0−1 μM.
(47) van der Schee, H. A.; Lyklema, J. *J. Phys. Chem.* **1984,** *88,* 6661.
(48) Donath, E.; Walther, D.; Shilov, V. N.; Knippel, E.; Budde, A.; Lowack, K.; Helm, C. A.; Möhwald, H. *Langmuir* **1997,** *13,* 5294.
(49) Caruso, F.; Lichtenfeld, H.; Donath, E.; Möhwald, H. Manuscript in preparation.
(50) Caruso, F., unpublished data.